Orbit-following fusion alpha wall load simulations for ITER including full orbit effects

T. Kurki-Suonio, O. Asunta, T. Koskela, S. Sipilä, A. Snicker, and S. Äkäslompolo
Aalto University, Association Euratom-Tekes, P.O. Box 14100, FI-00076 AALTO, Finland

Abstract

The accuracy of numerical evaluation of fast ion caused wall load for burning ITER plasmas is improved by introducing the possibility of following the full gyro orbits when necessary. The wall load in MHD quiescent plasma is calculated for ITER Scenario-4 in three different ways to assess the importance of the finite Larmor radius of alpha particles: 1. with pure guiding-center method, 2. with pure gyro-orbit following, and 3. with a hybrid method, where full-orbit following is evoked in the proximity of plasma-facing components. Is is found that, with ripple levels of acceptable magnitude, the wall load arising from simulations with finite orbit effects differ from the one obtained by traditional guiding centre estimates.

1 Introduction

The 3.5 MeV alpha particles, produced in large quantities in fusion reactions, present a potential hazard to the material structures that provide the containment of the burning plasma. In axisymmetric plasmas, these high-energy ions can be assumed to be well confined even with their large Larmor and banana radii. However, the finite number (18 in ITER) and limited toroidal extent of the Toroidal Field (TF) coils cause a periodic variation of the toroidal field, the magnetic ripple. This ripple enhances transport via finite orbit sizes and can provide a significant channel for fast particle leakage, leading to very localized fast particle loads on the walls. To prevent this, ferromagnetic inserts (FI) will be embedded in the double wall structure of the ITER vacuum vessel in order to reduce the ripple. Unfortunately, the breaking of the axisymmetry in ITER does not stop here. The neutral beam ports do not allow FIs at that location, leading to a locally enhanced ripple, and the presence of discrete ferromagnetic structures, such as the test blanket modules (TBM), cause poloidally and toroidally localized perturbations to the magnetic field. We shall refer to these local perturbations as 'field bump' to distinguish it from the global toroidal ripple exhibiting the 18-fold symmetry of the toroidal field coils.

The first numerical estimates for wall loads in the presence of the toroidal field (TF) ripple [1, 2, 3] were carried out with guiding centre (GC) integration [4, 5]. Not much later, it was, however, noted that the guiding centre approximation is valid only for devices of low or moderate aspect ratio and low TF ripple strength. In the devices outside this category, guiding centre approximation has to be relaxed and a full integration of the Lorentz force law is needed [6, 7]. From now on this is referred as Full Orbit (FO) integration.

In this paper, we present fusion alpha wall loads in ITER Scenario-4 obtained by FO integration using the ASCOT code [3]. We compare the results from simulations where the gyro orbits of alphas have been followed with FO for the full slowing-down time to full GC simulations as well as to the results from a hybrid scheme where FO is evoked only in the proximity of the first wall. To assess the effect of TF ripple, its magnitude is altered: we simulate a case with unmitigated ripple (no FI), a case with the ITER 2008 design, and the present case with the 2010 design. All simulations use the up-to-date first wall configuration with a 'continuous' limiter. Before showing the results, we introduce the full orbit integrator.

2 The orbit following and wall collision model in ASCOT

One of the key features of the Monte Carlo orbit-following code ASCOT is its capability to use fully 3D magnetic field and wall data of real tokamaks. The collisions are implemented with Monte Carlo operators, and particles are followed beyond the separatrix all the way to the vacuum vessel walls. There are three different ways to integrate the orbits. The GC integration, based on 5th order adaptive Runge-Kutta method, can be carried out in either Boozer coordinate system (1) or in Cartesian coordinate system (2) [4]. (The former is, however, limited inside the separatrix.) The third method is the FO integration scheme (3), presented in detail in Ref. [8]. The full orbit method used at the moment is a leap frog Boris method [9, 10] that integrates the equation of motion given by the Lorentz force,

$$\frac{d\mathbf{v}}{dt} = \frac{q}{m}\left(\mathbf{E} + \mathbf{v} \times \mathbf{B}\right), \tag{1}$$

and the equation for the particle position,

$$\frac{d\mathbf{x}}{dt} = \mathbf{v}, \tag{2}$$

where $\mathbf{v}$ is the velocity of the particle, $\mathbf{E}$ the electric field, $\mathbf{B}$ the magnetic field, m the mass and q the charge of the particle.

The leapfrog Boris method is found to work well: no orbit drift is observed and the energy is conserved. The magnetic moment is found to oscillate along the gyro orbit, but does not drift.

We use three different ways to check where the integrated orbit path has intersected a 3D wall element. In every case we use the raypolygon collision [11] for finding the possible intersection of a straight line and one of the wall segments that, in our case, can be triangles or quadrangles. This method is widely used in computer graphics applications and it has been further optimized for use in ASCOT. The most common way to deduce the point for wall collision is just to check where the line between two guiding centre points intersects wall segment. This will be referred pure GC check. Clearly this check is quite inaccurate and, in the case of complicated wall structures, even incorrect as it does not take into account the finite Larmor radius of the particle.

The second way to evaluate the wall collision point is to make a transition from GC integration to FO integration when the particle is one Larmor radius away from the nearest wall element. The transition is fully described in Ref. [8]. Since the evaluation of the distance to the nearest wall element is rather time consuming, the distance to

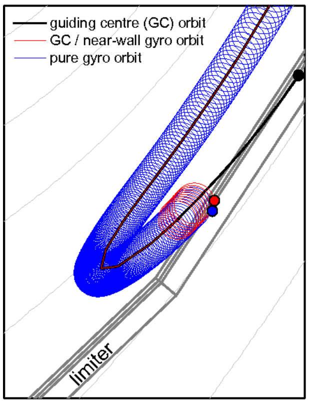

Figure 1: Due to the large Larmor radius of fusion alphas, guiding-center (GC) simulations do not give an accurate picture of alpha wall loads. By switching to full orbit (FO) simulation within a Larmor radius of the wall, more accurate load profiles are obtained at minimal CPU cost. In this figure, a guiding-center wall collision (black dot) is compared to a full gyro-orbit wall collision (blue dot), and to a hybrid model (red dot).

wall element is only calculated, when the particle is one Larmor radius away from the separatrix. When an ion guiding-center is found to be within a Larmor radius from a wall element, the latest guiding-center time step is cancelled and repeated by following the full orbit. The ion position is initialized using a random gyro angle. Full orbit simulation is then continued until the ion either hits a wall element or its guiding-center recedes beyond a Larmor radius from the nearest wall element, in which case the guiding-center model is again adopted in order to save CPU time. The switch to the guiding-center position can be made without introducing spatial error by solving the guiding-center equations of motion along with the full orbit equations. In the contrast to the full FO -method, the CPU time of this method is comparable to ordinary GC simulation. This method is dubbed the GC+FO -method.

Finally, the pure FO integration is the ultimate way for the wall collision check. It has been found to be about 70-100 times more CPU-intensive than the traditional GC method, and thus it appears to be an exaggerated tool for this purpose. However, for the complete FO simulations there are additional motivations besides the behaviour of the fast ions in the proximity of the first wall: In order to properly take into account the full orbit radial transport mechanisms that are not seen by the guiding-center formalism [6] in the presence of magnetic perturbations such as toroidal field ripple, the pure FO method must be adopted.

The different integration methods near ITER first wall are illustrated in Fig. 1.

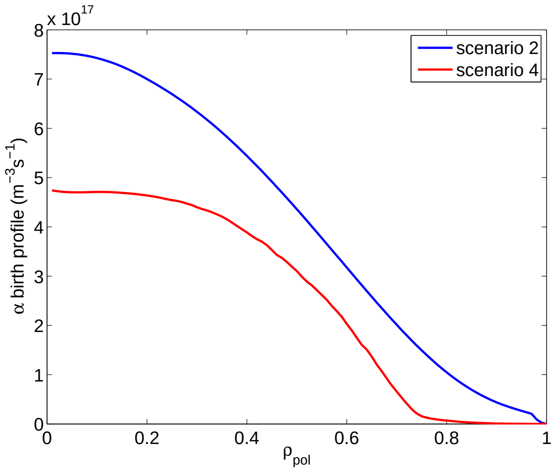

Figure 2: The birth profile of fusion alphas in Scenario-4, indicated by the red curve. The alpha source is strongly localized to the center so that practically no alphas are born outside $\rho > 0.75$.

3 Simulation results

The simulations are carried out for ITER Scenario-4, which is an advanced H-mode approaching steady state conditions. This is accomplished by reversed central shear that requires reduced plasma current of $I_p = 9$ MA. The lower current translates into wider orbit widths and, therefore, Scenario-4 is considered particularly vulnerable to perturbations in the magnetic field that can increase radial transport. The central density is 0.72×10^{20} m^{-3}, the central temperature 24 keV, leading to the fusion alpha birth profile indicated in Fig. 2. The background plasma includes the species D, T, He, ^{3}He, Be and Ar. Figure 3 shows the maximum field perturbation along the separatrix with and without the effect of ferritic inserts. The maximum ripple strength along the separatrix for unmitigated ripple is $\delta = 1.1\%$, and it is reached slightly above the outer midplane. The ferritic inserts reduce this value down to 0.25%, while the local field bump at the location of the neutral beam port reaches about 0.57 %, and the TBM-induced field bump is about 1.1 %.

In the simulations, 50000 ... 100000 3.5 MeV test alphas are initialized on a 2cm x 2cm grid, weighted by the local fusion rate and volume, and they are followed until they either intersect a first wall component or are slowed down below 100 keV, at which point they can be considered as part of the Maxwellian tail of the thermal population.

3.1 No FI: unmitigated ripple

Figure 4 shows the peak power loads to the wall from the three different cases, all for the most recent wall configuration, the 'continuous limiter' design, when no ferritic inserts to reduce the ripple are present. All the power is found to go to the limiters, regardless of the integration scheme. This is due to the high level of ripple that brings out the trapped alphas at such a high rate that the collisions with the background do not have enough time to transform the orbits sufficiently to allow entering the divertor region at around $\theta > 100°$. There are two areas of major deposition on the low-field side: the large

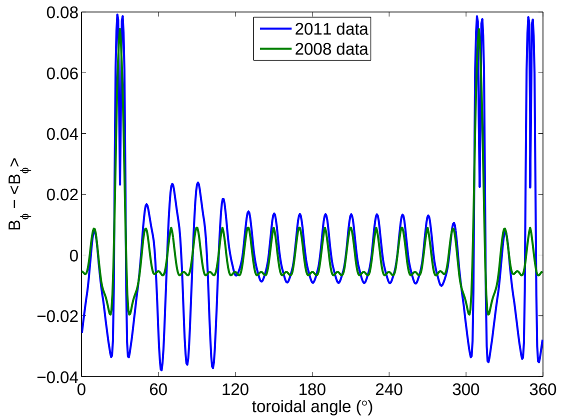

Figure 3: The maximum field perturbation on the separatrix as a function of the toroidal angle. The blue line stands for the case with the most recent design FI design, while the green line stands for the 2008 design. The three distinct peaks correspond to the perturbation due to the TBM, while the local increase in the ripple strength at around 50° – 120° is due to the absence of the inserts at the location of the neutral beam port.

peak right below the midplane is because the trapped orbits are widest there and the magnetic geometry such that it is ions approaching the midplane from below that are still increasing their radial excursion. The second peak, in the region 35° – 70° below the midplane, appears because it is there that the plasma is closest to the wall. The double-hump structure is due to the wall tiles being straight and at an angle with respect to each other, thus forming a region further away from the plasma that is practically inaccessible to fast ions.

The peak heat flux reaches MW-range, making FIs absolutely necessary.

3.2 The 2008 FI design

Figure 5 shows the peak wall power load on the 'continuous limiter' design when the ferritic inserts of the 2008 design reduce the ripple. The wall power loads are reduced by almost two orders of magnitude. Practically all the power is still found on the limiters, regardless of the integration scheme, but in this case the area around the midplane dominates. Here the choice of the integration scheme is found to make a difference: the peak power load calculated by FO following is about five times larger than the one obtained by GC following, and altogether about twice as high as with the GC+FO method.

The maximum peak power loads of tens of kW/m^2 are easily tolerated by the wall materials.

3.3 The 2010 FI design

Figure 6 shows the peak wall power load on the 'continuous limiter' design when the ferritic inserts of the 2010 design reduce the ripple. Only GC and GC+FO results were available at this time, but pure FO-following results are not likely to reveal information

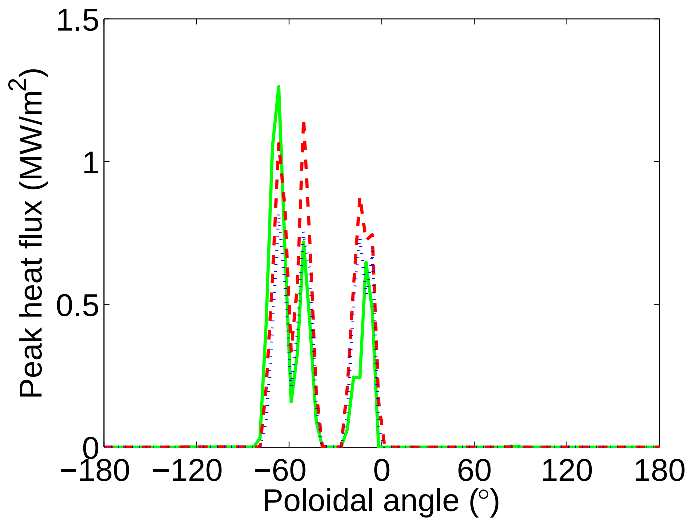

Figure 4: The peak power load distributions given by the three different integration schemes in the absence of any ferritic inserts to reduce the ripple level. The blue line stands for the FO integration scheme, red for the FO+GC scheme, and green for the pure GC scheme.

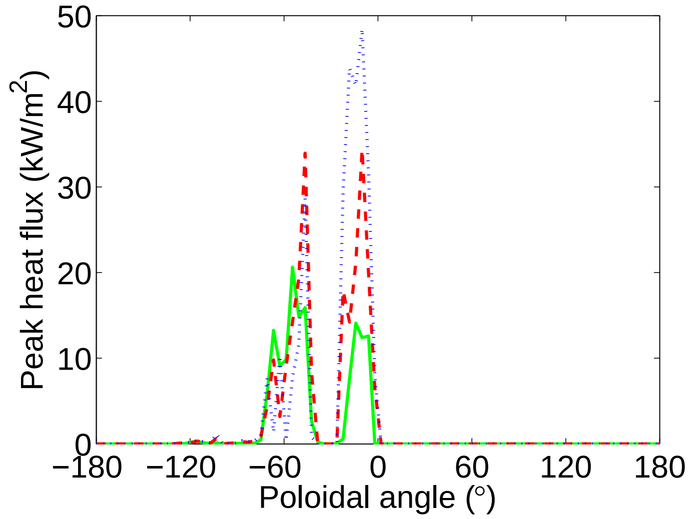

Figure 5: The peak power load distributions given by the three different integration schemes in the presence of the 2008 design of the FIs to reduce the ripple level. The color coding is the same as in Fig. 4.

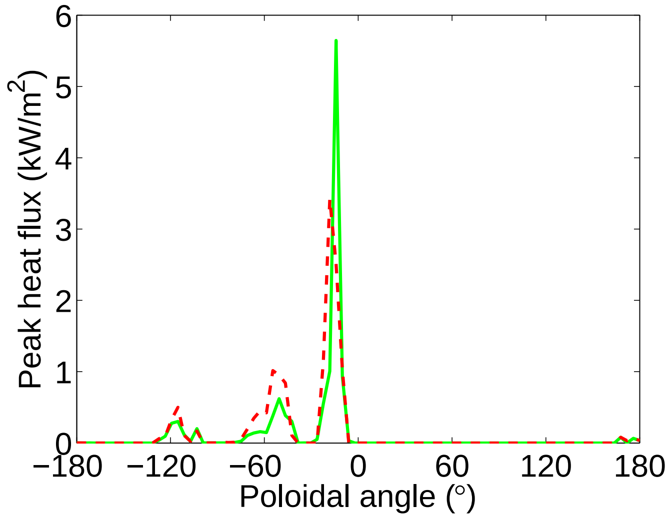

Figure 6: The peak power load distributions given by guiding-center and hybrid integration schemes in the presence of the 2010 design of the FIs to reduce the ripple level. The color coding is the same as in Fig. 4

of any significance. This is because the peak power loads are further reduced by almost an order of magnitude, so that the maximum fluxes are now measured in kW/m^2. The midplane area dominates the load, but due to the strongly reduced ripple transport even the divertor region is now found to receive some power when the ions can slow down and their orbits become sufficiently narrow to enable them to penetrate to the divertor.

4 Conclusions and future work

In our continuing effort of obtaining ever more quantitatively reliable estimates for fast ion power loads on ITER first wall, we have upgraded the Monte Carlo orbit-following code ASCOT so that, in addition to accommodating 3D magnetic structures and first wall geometries, it now also allows choosing between the guiding-center formalism and gyro orbit following.

The simulations were carried out for ITER Scenario-4 using the most recent first wall design with 'continuous' limiter, i.e., poloidally extended limiter plates between each coil pair. The wall loads were calculated with three different integration schemes: pure full orbit following, pure guiding center following, and hybrid method, where guiding center following was switched to full orbit following close to the wall. This was done for three different magnetic geometries: 1. unmitigated ripple, 2. ripple reduced with the 2008 FI design, and 3. ripple reduced with the 2010 FI design.

The unmitigated ripple results in unacceptably high peak power loads on the wall, measured in MW/m^2. The ferritic inserts bring the peak wall loads down to tens of kW/m^2 with the 2008 design, and to a few kW/m^2 with the 2010 design. Larmor radius effects were found important for the power distribution on the wall when the ripple was mitigated by FIs. We calculated the wall distribution using three different ways of evaluating the location where an ion intersects a material surface. The methods differed in the degree to which they accounted for the finite Larmor effects, with varying cost in CPU consumption. It was found that pure guiding-center approach gives misleading wall distributions and, consequently, gyro orbits should be followed in the vicinity of the first wall. Qualitatively, all simulations including Larmor effects gave similar results.

In conclusion, with ripple mitigation by FIs, the wall power loads by fusion alphas were found insignificant as far as material integrity is concerned. However, it should be kept in mind that these results were obtained neglecting any fast ion transport processes aside from the collisional neoclassical transport. This is highly idealistic, since fast ion related MHD is bound to be present in ITER and affecting the fast ion population. If e.g. some Alfvenic activity redistributes the now centrally localized high-energy alpha population further towards the edge, the results are expected to change dramatically when additional transport processes, induced by 3D field aberrations, rapidly take the ions to the first wall components.

Acknowledgements.
This work was partially supported by the Academy of Finland Projects No. 121371 and 134924, and the European Communities under the contract of Association between EURATOM/TEKES. The simulations were done using the computational facilities of CSC, the Finnish IT Center for Science and resources at HPC-FF.

References

[1] M. Redi *et al.*, Phys. Plasmas **3** (1996) 3037

[2] K. Tani K. *et al.*, IEEJ Trans. on Fundamentals and Materials **125** (2005) 938

[3] T. Kurki-Suonio *et al.*, Nucl. Fusion **49** (2009) 095001

[4] X. Tao, A. A. Chan and A. Brizard, Phys. Plasmas, **14** (2007) 092107

[5] R.B. White and M.S. Chance, Phys. Fluids **27** (1984) 2455

[6] H. Mimata *et al.*, Prog. in Nuclear Energy **50** (2008) 638

[7] K.G. McClements *et al.*, Phys. Plasmas **12** (2005) 303712

[8] A. Snicker, T. Kurki-Suonio, S. Sipilä, Transactions in Plasma Science, 38(9) (2010) 2177

[9] H. X. Vu and J.U. Brackbill, J. Comput. Phys., **116** (1995) 382

[10] P. Degond *et al.*, C. R. Acad. Sci. Paris, Ser. I **343** (2006) 613

[11] D. Badouel, An efficient ray-polygon intersection. In A. S. Glassner (ed.), Graphics Gems, pp. 390–393, (1993) Academic Press, Boston (MA)